DIAGNOSTIC NUCLEAR MEDICINE

Clinical Validation of Fully Automated Computation of Ejection Fraction from Gated Equilibrium Blood-Pool Scintigrams

Johan H. C. Reiber, Swan Peng Lie, Maarten L. Simoons, Cees Hoek, Jan J. Gerbrands, William Wijns, Willem H. Bakker, and Peter P. M. Kooij

Erasmus University and University Hospital Dijkzigt, Rotterdam, Delft University of Technology, The Netherlands

A fully automated procedure for the computation of left-ventricular ejection fraction (EF) from cardiac-gated Tc-99m blood-pool (GBP) scintigrams with fixed, dual, and variable ROI methods is described. By comparison with EF data from contrast ventriculography in 68 patients, the dual-ROI method (separate end-diastolic and end-systolic contours) was found to be the method of choice; processing time was 2 min. Success score of dual-ROI procedure was 92% as assessed from 100 GBP studies. Overall reproducibility of data acquisition and analysis was determined in 12 patients. Mean value and standard deviation of differences between repeat studies (average time interval 27 min) were 0.8% and 4.3% EF units, respectively, ($r = 0.98$). We conclude that left-ventricular EF can be computed automatically from GBP scintigrams with minimal operator-interaction and good reproducibility; EFs are similar to those from contrast ventriculography.

J Nucl Med 24: 1099–1107, 1983

Technetium-99m equilibrium gated blood-pool scintigraphy permits visualization of the distribution of a radioactive tracer in the heart chambers as a function of time within a representative heart cycle. After appropriate background subtraction, the total number of counts within the left ventricular (LV) region of interest (ROI) in the LAO 45° projection, usually modified with a 10° caudal tilt, provides a direct measure of instantaneous LV volume (*1,2*). Computation of the global and regional ejection fractions (EF) thus requires the delineation of the LV boundary and the definition of a region for background correction. This may be achieved by manual tracing of the outlines or by means of a semi- or fully automated edge-detection algorithm (*3–10*). The manual procedure is characterized by relatively large inter- and intra-observer variations, which hamper the assessment of effects of interventions, such as exercise, on ejection fraction (*11,12*).

Received Feb. 16, 1983; revision accepted July 18, 1983.

For reprints contact: Dr. Johan H. C. Reiber, Laboratory for Clinical and Experimental Image Processing, Thoraxcenter, Erasmus University and Hospital Dijkzigt, Rotterdam, The Netherlands.

The "ideal" analytical procedure should combine the following characteristics: (a) similarity between scintigraphic EF and the EF obtained from contrast ventriculograms under similar physiologic conditions; (b) basically fully automated, although permitting user intervention at various crucial steps; (c) a high success score of the fully automated mode under routine clinical conditions; and (d) the procedure must be computationally fast. Since no commercial software package satisfying these conditions was available at the start of our project in 1980, we set out to develop one. This implied investigating the effects on the EF of different methods for the definition of the LV and background ROIs.

Accordingly, we have devised algorithms for the fully automated contour detection of the LV activity structure in (a) the sum image of the study (fixed-ROI method), (b) the separate end-diastolic (ED) and end-systolic (ES) images (dual-ROI method), and (c) each of the separate frames of the study (variable-ROI method) (*13–15*). Background correction is achieved through automated selection of an "optimal" background region.

Although the analytical procedure is fully automated, it permits user interaction at various crucial steps. This procedure has been implemented on a computer system.*

It was the purpose of this study to determine which of the implemented methods correlates best with the ejection fractions from single-plane radiographic ventriculography, using 68 patient studies. In addition, the reproducibility of the gated blood-pool data acquisition and subsequent analysis was determined from a group of 12 patients who were studied twice. Finally, the need for operator interaction during the analysis was evaluated in 100 consecutive resting gated blood-pool studies.

PATIENT SELECTION AND METHODS

Gated blood-pool scintigrams and single-plane contrast LV cineangiograms were analyzed from 68 adult patients (60 male and eight female) who were referred for diagnostic cardiac catheterization. Median delay between scintigraphic and contrast studies was 2 days (range 0–45 days). Contrast ventriculography was performed in 30° RAO projection and the ejection fraction was computed by the area-length method from manually traced end- diastolic and end-systolic contours.

Gated blood-pool scintigrams were obtained at rest with a 6-min acquisition protocol, using in vivo RBC labeling with 15 mCi (555 MBq) technetium-99m. Gated scintigrams (20 frames per cycle) were collected in the LAO 45° view, usually with a 10° caudal tilt, and the LAO 65° and RAO 25° views. Data were collected in zoom mode (64 × 64 matrix), with a magnification factor of two in 48 patients and of $\sqrt{2}$ in 20 patients, using a medium-field (25 cm field of view) gamma camera. A low-energy, all-purpose (LEAP) collimator was used in 53 patients and a high-sensitivity (HS) collimator in 15; all HS studies were acquired with a zoom factor of two. In the $\times\sqrt{2}$ zoom mode each pixel represents a square with ~2.8-mm sides, in the ×2 zoom mode the square is ~2 × 2 mm. Automated detection of the LV boundary was performed in the LAO 45° projection.

The reproducibility of the entire procedure of data acquisition and analysis was assessed from a group of 12 patients (11 male and one female), who were studied twice in the LAO 45° orientation with an average interval of 27 min (range 15–50 min). Studies used the LEAP collimator and a zoom factor of two. The first study was performed at the beginning of the diagnostic procedure; the second followed data acquisition in the anterior and LAO 65° views. After the third view had been completed, the patient was asked to leave the camera bed for a few minutes, after which the second LAO 45° study was performed. Thus the positioning of both camera and patient had to be completely redone.

Since operator intervention is permitted (e.g., modification of automatically chosen contours), the need for such intervention was evaluated in a series of 100 consecutive patients referred for gated blood-pool scintigraphy.

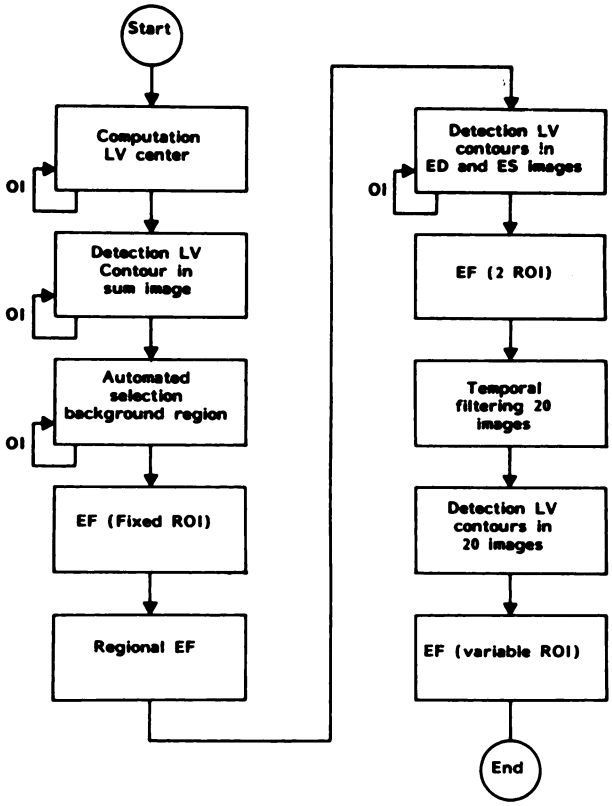

FIG. 1. Flow diagram for automated analysis procedure for computation of ejection fraction by three different methods.

A flow diagram of the procedure for the computation of the ejection fraction by the three methods is shown in Fig. 1 (for details see Appendix). The algorithms have been published elsewhere (*13–15*). The procedure starts with the determination of the approximate center of the LV activity in the first frame of the study. The LV contour is then first detected in the sum image with a minimum cost contour detection algorithm. The center position is then updated using the centroid of the bounded LV activity structure, and the contour detection process is repeated, yielding the final LV contour (*14,15*). An "optimal" background region is then selected from a total of six regions, generated in directions from 1 through 6 o'clock relative to the LV center. This "optimal" background region is selected on the basis of the mean value and the variance of the background activity as a function of time in each region (see Appendix). The LV time-activity curve is corrected for background, and the end-diastolic and end-systolic frames are determined. From these data the ejection fraction is computed by the fixed-ROI method.

Subsequently, the LV contour is divided into six 60° sectors centered on the LV structure, and for each sector the regional ejection fraction is computed.

For the dual-ROI computaion of EF, new ED and ES

TABLE 1. LEFT VENTRICULAR AND BACKGROUND COUNT DENSITIES AVERAGED OVER ALL STUDIES IN THE THREE DIFFERENT GROUPS

	LEAP coll. zoom × 2 (n = 33)	LEAP coll. zoom × $\sqrt{2}$ (n = 20)	HS coll. zoom ×2 (n = 15)
LV counts/pixel in ED frame:			
average	31.7	40.2	51.9
s.d.	11.0	15.9	12.3
Background counts/pixel			
average	16.6	21.2	26.3
s.d.	5.3	9.7	6.6

images are defined by the weighted sum (1-2-1) of neighboring frames of the known ED and ES frames, respectively. Applying the same contour-detection technique, the ED and ES contours are established in these ED and ES images. The "optimal" average background count/pixel is subtracted, and ejection fraction by the dual-ROI method is computed.

Before the automated detection of the contours in the separate images of the study, the frames are filtered temporally with weighting factors 1-2-1. Finally, the contours in the separate frames are detected with the minimum-cost contour algorithm (Appendix). To guide the search of the contour in frame m, an expectation window is defined, based on the detected contour in frame m-1. From the net time-activity curve, the ejection fraction by the variable-ROI method is determined.

Using Student's t-test for paired values, the results were analyzed for significant differences between the different methods.

RESULTS

To obtain a measure of the count densities in the images, for each patient study we computed the average number of LV counts per pixel within the ED contour in the ED frame, as determined by the dual-ROI method; also the average background count per pixel within its "optimal" background region. The gross LV counts were measured within the original ED frames; the background counts have been averaged over the first 14 frames of the study (see Appendix). For the overall mean values and standard deviations of these count densities, three groups of studies have been distinguished, depending on the collimator and zoom factor applied (Table 1). Using the unpaired t-test, no significant differences between the ratios of average LV and background counts/pixel were found for the three groups.

Figure 2 (top-bottom) presents the scatter diagrams of the LVEF data obtained by radiographic angiography

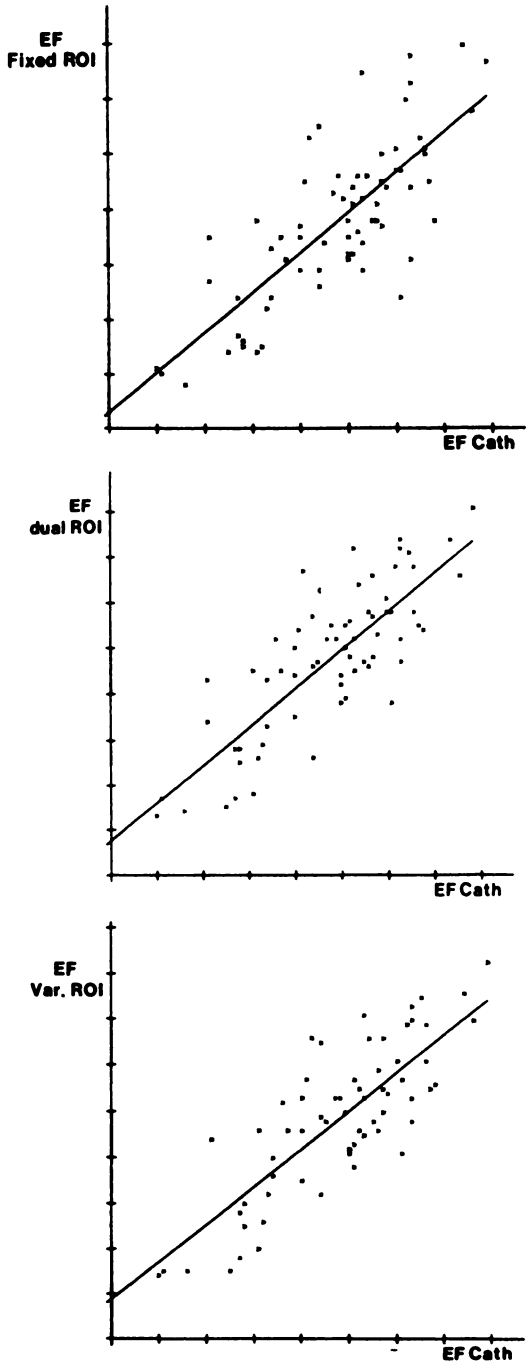

FIG. 2. Scatter diagrams for scintigraphic EF using fixed ROI (2, top), dual ROI (2, center), and variable ROI (2, bottom), plotted against the results from contrast angiography. Solid lines represent regression equations.

compared with those computed by the three scintigraphic methods for the entire group of 68 patients. Heart rates were similar during the two studies. In order to facilitate this comparison of the three methods, the mean difference and the standard error of the estimate (s.e.e.) between the scintigraphic and contrast EF results are presented in Table 2 for each method, the numbers representing EF units as percentages. The mean difference is defined as the mean value of the individual dif-

TABLE 2. COMPARISON OF EJECTION FRACTION FROM CONTRAST VENTRICULOGRAPHY WITH EF USING THREE DIFFERENT ROI METHODS

	Fixed ROI	Dual ROI	Var. ROI
Mean diff.	9.8	0.1	−0.8
p-value*	$<2 \times 10^{-11}$	n.s.	n.s.
s.e.e.	9.2	9.5	9.7
Correlation coeff.	0.78	0.81	0.80
Intercept	3.0	7.6	8.8
Slope	0.73	0.84	0.83
Computation time (sec)	70	120	185

* Student's t-test for paired values.

Regression equation: $EF_{ROI} = \text{slope} \times EF_{contrast} + \text{intercept}$.

TABLE 3. COMPARISON OF SIZES OF END-DIASTOLIC LEFT-VENTRICULAR ROIs BY THREE ROI METHODS (MEAN ± s.d.)

	Fixed ROI	Dual ROI	Var. ROI
LEAP coll., zoom 2X	780 ± 213	908 ± 225	887 ± 215
	$p < 2 \times 10^{-10}$	n.s.	
	$p < 2 \times 10^{-6}$		
LEAP coll., zoom $\sqrt{2x}$	399 ± 113	464 ± 116	455 ± 115
	$p < 4 \times 10^{-10}$	n.s.	
	$p < 9 \times 10^{-7}$		
HS coll., zoom 2X	932 ± 206	1027 ± 203	1027 ± 202
	$p < 3 \times 10^{-5}$	n.s.	
	$p < 3 \times 10^{-4}$		

ferences ($EF_{cont} - EF_{scint}$). The regression equations and the correlation coefficients are also given, and the computation time for each analysis procedure. A histogram of the automatically selected background directions for the 68 studies is given in Fig. 3.

For each patient study, the number of LV pixels within the detected ED ROI was computed for the three ROI methods. It is clear that with a fixed ROI the ED ROI equals the single ROI detected in the sum image. The same three groups of studies as defined in Table I were distinguished, depending on the collimator and the zoom factor applied. The overall mean values and standard deviations are listed in Table 3. For all three groups of studies, significant differences were found between the number of LV pixels within the fixed ROI and those within the dual- and variable-ROI methods; the numbers of LV ED pixels as determined by the dual- and variable-ROI methods were not significantly different.

Table 4 presents the mean values and standard deviations of the differences of the repeated measurements for the fixed- and dual-ROI methods, along with the regression equations and correlation coefficients. The data were obtained from fully automated analyses of patient studies without any operator interaction. These results show that the mean differences between repeated studies were only 0.3 and 0.8 EF units (%) for the fixed- and dual-ROI methods, respectively. The corresponding standard deviations of the differences, 3.7 and 4.3, are considerably smaller than the values found in the comparison with the radiographic left ventriculography data. The linear regression equations for the fixed- and dual-ROI methods are $y = 1.06\,x - 1.5$ and $y = 1.09\,x - 2.8$, respectively; the correlation coefficients for both methods are 0.98.

Required operator interaction in the routine analysis

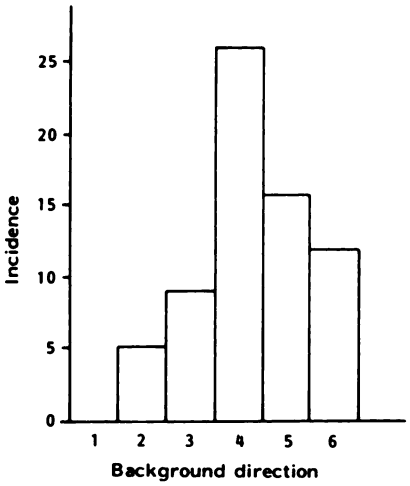

FIG. 3. Histogram of automatically selected background directions for 68 patients studies.

TABLE 4. REPRODUCIBILITY OF ENTIRE DATA ACQUISITION AND ANALYSIS PROCEDURE

	Fixed ROI	Dual ROI
Mean diff.	0.3	0.8
p value*	n.s.	n.s.
Standard dev. of diff.	3.7	4.3
Correlation coeff.	0.98	0.98
Intercept	−1.5	−2.8
Slope	1.06	1.09

Regression equation: $(EF_{study})^1 = \text{slope} \times (EF_{study})^2 + \text{intercept}$.

* Student's t-test for paired values.

of the gated blood-pool scintigrams has been assessed from a group of 100 consecutive resting studies. The median value of the dual-ROI EF for this group was 55% with a range of 13-80 EF units. Table 5 presents the success scores for the various sequential steps in the entire analysis. The analysis procedures were all judged by two experienced observers, who decided on a consensus basis whether they could agree with the various results or not. The success score for the variable-ROI method was assessed from a subset (n = 48) of the total of 100 studies; in this case the observers disagreed only in three studies (6%) with one or more of the total of 20 detected contours per study.

Computation of the dual-ROI EF value requires the definition of the ED and ES frames on the fixed-ROI LV time-activity curve. Therefore, determining the success score for the dual-ROI EF measurement must include the various steps from both the fixed- and dual-ROI methods. The overall success score for the dual-ROI measurement was 92%. Three of the eight studies for which a correction had to be applied had a dual-ROI EF value below 55% (range 33–49), whereas the other five studies had a dual-ROI EF above 55% (range 56–75).

The programs have been implemented on a minicomputer system* with hardware floating-point processor and cache memory. The computation time for the EF measurement by the fixed-ROI method was 70 sec, and an additional 50 sec were needed for the dual-ROI method (Table 1). The variable-ROI method (new sum image + 20 frames) requires 115 sec more than the fixed-ROI method. The fixed-ROI method is always run first to allow determination of the LV center position and the optimal background region. All programs run under the F/B monitor with 14K words occupied by the program.

TABLE 5. SUCCESS SCORES OF VARIOUS STEPS IN IMPLEMENTED LVEF ANALYSIS ASSESSED FROM 100 CONSECUTIVE REST STUDIES

	Success score
Initial LV center position	98%
LV contour in sum image	97%
LV ED contour	100%
LV ES contour	94%
LV ED and ES contours	94%
LV contours in variable-ROI method (n = 48)	94%
Overall fixed + dual-ROI methods	92%

DISCUSSION

Technetium-99m equilibrium gated blood-pool scintigraphy to date is a widespread noninvasive procedure that allows measurement of important parameters of LV function. Since the LV counts are a measure of LV volume, no geometric assumptions have to be made for the calculation of ejection fraction, in contrast to the assessment of EF from radiographic left ventriculograms (*1*,*2*). The computation of scintigraphic EF requires the definition of LV region(s) of interest encompassing the LV activity structure, and of a background region. Unfortunately, the values obtained for EF following the various techniques may differ substantially. In routine clinical practice, the analysis procedure should fulfill several conditions: (a) the scintigraphic EF should agree with EF values obtained from contrast ventriculograms under similar physiologic conditions; (b) the procedure should show low inter- and intra-observer variations to appreciate small changes during intervention studies, which demand an automated computerized analysis; (c) the automated procedure must be characterized by a high rate of success under different conditions of image quality; and (d) the computation must be rapid.

Because of its high-resolution images and its relatively long history, radiographic left ventriculography has been generally accepted as the "gold standard" for the computation of the EF, despite its known limitations such as the geometric model that must be assumed and the inter- and intraobserver variations in the EF results. Since the gated blood-pool technique also attempts to provide ejection fraction data, although based on different principles, for routine clinical practice one should use the particular ROI method that provides EF data similar to those obtained from contrast ventriculography.

Numerous ways have been developed to define LV and background ROIs, with widely varying results in EF (*16–19*). In an earlier study we investigated the effect on EF of five different methods for background selection (*15*). At that time, the initial LV center was still chosen manually by the operator. The five background methods were: (a) fixed at 3 o'clock; (b) in a user-defined direction; (c) automatically selected on the basis of the mean and variance of the background time-activity curve; (d) defined by the difference in area between the ED and ES contours; and (e) no background correction at all. It appeared from that preliminary study that the automated selected background would be preferable. The histogram of Fig. 3 shows that in most cases the background direction is selected in the lower right quadrant of the image (between 4 and 6 o'clock). This is in accordance with the recommendations by the Working Group of Nuclear Cardiology of the European Society of Cardiology (*20*). Because of these findings we have applied the automated background selection procedure for the present comparison of the three different LV ROI methods.

In the present study slightly different acquisition protocols have been used. Table 1 shows that the count

densities for the LEAP collimator with a zoom factor of $\sqrt{2}$ increase by nearly this factor compared with those studies with a zoom factor of 2, although at the expense of spatial resolution. The count densities with the HS collimator increase by a factor of ~1.6 relative to the LEAP studies with the same zoom factor, which is advantageous for stress studies and automated edge-detection purposes. No significant differences in the ratios of average LV and background counts per pixel were found between the three groups.

From the data in Table 2 (mean values and s.d. of the differences between the scintigraphic and radiographic contrast procedures for the three LV ROI methods, assessed from all 68 patient studies) it appears that the best results are obtained with the dual-ROI method. Its differences with the radiographic method are not significant, and the rather large s.e.e. can be blamed partly on the substantial interobserver differences in the "gold standard" itself (*21*,*22*). We feel, accordingly, that the dual-ROI and the radiographic methods are equivalent, and our preference for dual ROIs is shared by Bacharach et al., who also favor the use of both ED and ES contours if the ES ROI can be determined in a highly reliable manner—as by an automated edge-detection scheme (*23*).

The fixed-ROI scintigraphic method underestimates the EF by an average of 9.8 EF units compared with radiographic ventriculography ($p < 2 \times 10^{-11}$), thus confirming the results from other authors (*18*, *19*, *24*, *25*). For one thing, during systole the atria and the right ventricle may move towards the left ventricle and partly overlap the single LV ROI, thus inflating the true ES counts. Second, it appears from Table 3 that the fixed ROI detected in the sum image is significantly smaller than the ROIs detected in the end-diastolic frames by the dual-ROI and variable-ROI methods. This means that the ED contribution measured with fixed ROI may underestimate the true ED counts. No significant differences in the sizes of the ED contours were found between the dual-ROI and variable-ROI methods. The smaller fixed-ROI sizes may result because the systolic and diastolic frames contribute few counts along the ED boundary; the main density lies farther in. As a result, the maximal response of the second-derivative function may shift slightly towards the LV center along some radii, which can be shown by comparing cost matrices from ED and sum images. Despite these limitations, the fixed ROI serves a number of important functions as a preprocessing tool for the dual-ROI approach: (a) providing automated selection of ED and ES frames, and (b) because of the high count densities in the sum image, it yields a highly reproducible contour that serves as a guide for the six derived background regions.

It appears from Tables 2 and 3 that—aside from the computation times—the variable- and dual-ROI methods perform about equally well. For the computation of EF, the difference between the two methods is that for the detection of the ES ROI with variable-ROI, temporal information was used, based on the detected contours in the preceding frames. Such temporal information is not used for contour detection by the dual-ROI method. As a result, the ES contours by these two procedures may differ slightly, and therefore the EF values. However, the comparison with the contrast EF values shows that there are hardly any differences between the dual- and variable-ROI methods. Therefore, the variable-ROI method is rejected only because it is computationally more expensive (185 sec compared with 120 sec for the dual-ROI method).

Since the analysis is basically fully automated, with built-in arrangements for intervention if the operator does not agree with the intermediate results, the inter- and intraobserver variations for the same study are essentially zero. The results on the success score of the procedure indeed show that the method requires minimal interference. In those cases where the observers did not agree with the detected contours, only a small correction of the contour was necessary. The discrepancy occurred mostly at the apex of elongated left ventricles; because of the constraints built into the edge-detection algorithm, the detected contours tended to cut off the low-count tip of the apex. This error, however, has only a minimal effect on the ejection fraction.

The reproducibility of the analysis of two independent studies in 12 patients was excellent, with a mean difference for the fixed- and dual-ROI methods of 0.3 and 0.8 EF units (%), respectively, with standard deviations of 3.7 and 4.3 units. The correlation coefficient was 0.98. These results compare well with the results from Pfisterer (*26*), Slutsky (*27*), and Wackers (*28*).

In conclusion, our evaluation shows that LVEF can be computed automatically from gated blood-pool scintigrams with minimal operator interaction. The measured ejection fractions are similar to those from contrast ventriculography, and the method has an excellent reproducibility. Routine use of such methods is to be preferred over procedures that require manual delineation of LV and background regions.

FOOTNOTE

* DEC gamma-11.

ACKNOWLEDGMENTS

This work has been supported in part by the Dutch Heart Foundation under Grant No. 78,058. The authors thank Ria Kanters-Stam for her secretarial assistance.

APPENDIX

Automated processing of gated blood-pool scintigrams. Definition of LV center. To allow contour detection in polar coordinates, the LV center must be determined. This is done automatically in the first frame of the study. In this frame the 64 sums from the columns and rows are computed and smoothed with an unweighted

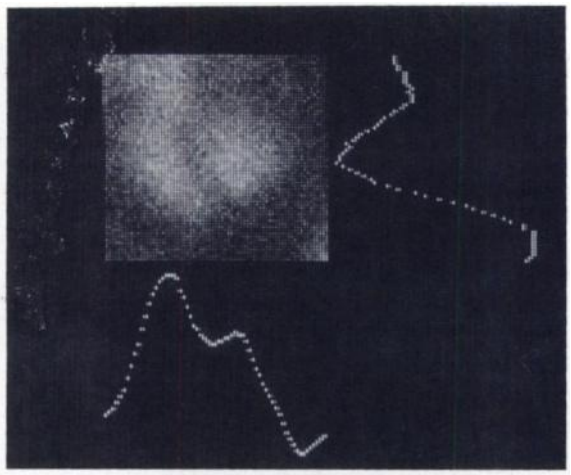

FIG. 4. Automated definition of approximate center of LV activity distribution from column and row sums.

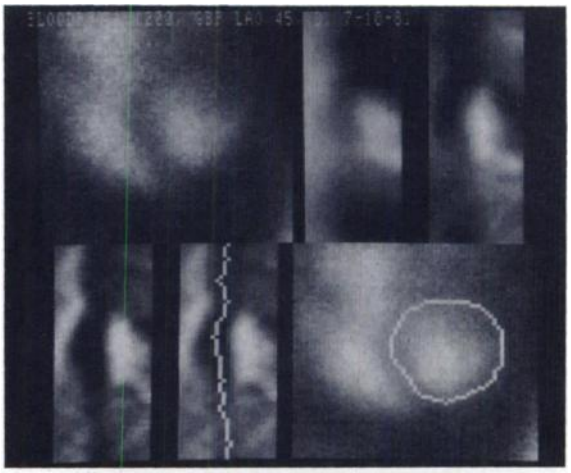

FIG. 5. Top images represent (left to right) original sum image, polar image, and first-derivative image. Bottom-row images represent (left to right) cost matrix, detected contour superimposed on cost matrix, and sum image with detected contour superimposed.

5-point operator. A provisional center position is found by searching the row and column sums at the right lower corner of the image for the first local maximum values above certain row and column thresholds, respectively. The threshold value, THRES, for the row or column sum has been found empirically to be:

$$\text{THRES} = (\text{MAX-MIN}) \times 4 + \text{MIN},$$

where MAX and MIN denote the absolute maximum and minimum values between the 11th and 54th positions of the particular vector, respectively. Figure 4 shows the first frame of a gated blood-pool study with plots of the row and column sums. Following the computation of this initial center position, a 21- by 21-pixel area, centered around this position, is defined. Next, the total count within a submatrix of size 7 × 7 is determined for each of the possible positions of the submatrix within the 21 × 21 area. The center position of this submatrix at the location with the maximal total number of counts is then assumed to be the approximate center of the LV activity structure. This provisional center does not necessarily coincide with the geometric center of the left ventricle or with its center of gravity. This does not pose a serious problem for the contour-detection algorithm, since this approximate center will be updated by the contour algorithm itself. The provisional center simply provides a starting point for further analysis. In case the algorithm fails to find a reasonable center position, the user may correct the position with the joystick of the computer system.

Automated contour detection. The principle of minimal-cost contour finding allows the detection of contours, even in images with poor S:N ratios (*29*).

Computation of a minimal-cost contour is generally very time-consuming. For our particular application, the procedure can be simplified by defining the following constraints:

1. The left ventricular contour is a simple, closed, and almost convex curve.
2. The contour is to be found within a circular belt defined by minimal and maximal distances from the center of the LV (expectation window).

These conditions can be incorporated into the detection procedure relatively simply once the image has been converted to polar coordinates. Searching for the contour then becomes simpler in that the contours always consist of a fixed number of points, which simplifies the definition of a cost function.

The polar representation is obtained by sampling the original image along 64 radii from the provisional center of the LV. Along each radius 32 samples are taken, with sample distances equal to the pixel spacing in the x,y matrix. The value of a pixel in the polar matrix is defined by the average of the 3 × 3 neighborhood of the pixel closest to the sample point in the original image. This polar representation is shown in Fig. 5 (top center) together with the original sum image (top left). The radial distance is plotted along the horizontal axis and the angular position counterclockwise with respect to the 3 o'clock direction in the x,y matrix is plotted along the vertical axis.

The detection of the edges in the polar image is achieved by means of a second-derivative operator applied along the horizontal lines in the polar image. The second-derivative image is obtained by applying a first-derivative operator twice. Finally, the cost matrix is defined as the inverse of the second-derivative image. The top right image in Fig. 5 is the first-derivative image and the bottom left image the cost matrix. The displayed brightness levels in the cost matrix are proportional to the cost coefficients. The band in which the contour is to be detected is characterized by low costs (low brightness levels), as can be seen in this image.

The minimal-cost contour is the minimum-cost path from the bottom to the top in this cost matrix (Fig. 5, bottom center). This minimum-cost path is found by means of a dynamic programming method. Retransforming to Cartesian coordinates and connecting the 64 contour positions results in a continuous contour (Fig. 5, bottom right).

It is clear that the detected contour will depend on the initially computed center position. Accordingly, this center position is now replaced by the centroid of the activity distribution within the initially generated contour and the contour-detection procedure is repeated from this centroid. Repetition of this procedure will converge toward an optimal center position, but in practice a single iteration suffices, since then the deviation from the optimal position is usually not more than 1 pixel in x- and/or y-direction. One iteration is therefore taken to give the final contour, which may then be used for the computation of the EF by the fixed-ROI method. The computation time for the foregoing procedure is only 12 sec.

If the user does not agree with the displayed contour, he may correct it or draw a new one with the joystick.

Background definition and computation of ejection fraction. Six background regions are generated in the six directions ranging from 1 to 6 o'clock around the LV center. These background regions are fixed in size and in distance from the LV boundary. In our routinely applied package, the region has a width of four pixels, a distance from the LV boundary of one pixel, and an angle of 45°. The time-activity curves for these six background regions are

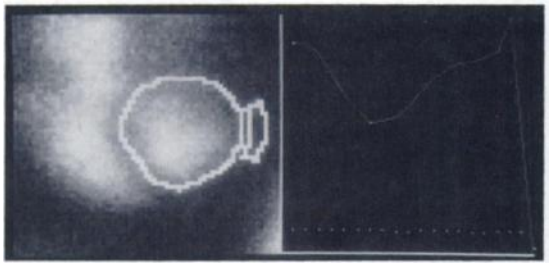

FIG. 6. Left: sum image with detected contour and defined background region superimposed. Right: background-corrected LV time-activity curve (fixed-ROI method). LVEF = 36%.

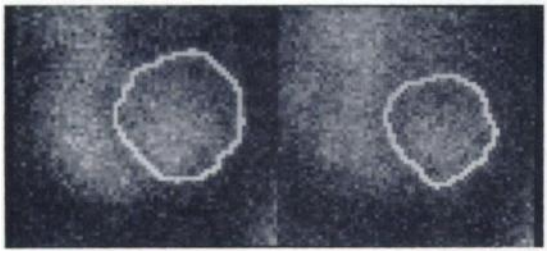

FIG. 7. End-diastolic (left) and end-systolic (right) images with detected contours superimposed (dual-ROI method). LVEF = 46%.

computed and the "optimal" background region is defined as that having minimal variance in the time-activity curve, selected from the three background regions showing the lowest mean activity. The number of frames involved in the computation of the variance is 14, representing the first 70% of the total number of frames of the study, thus avoiding the usual drop-off in counts in the last frames. From the selected background region, the overall average background count/pixel is computed from the 14 frames. The gross LV activity in each frame is then corrected using this average background. Figure 6 shows the results for this fixed-ROI method. The ED and ES frames are defined from the net LV time-activity curve by the maximal and minimum activity values. The fixed-ROI ejection fraction in this particular example was 36%.

Ejection fraction by the dual-ROI method. On average, the EF by the fixed-ROI method underestimates the ejection fraction computed by radiographic ventriculography, for the reasons given earlier. This discrepancy can be reduced by using separate ED and ES contours. To improve the S:N ratio in the ED and ES images, 1-2-1 weighted sums are computed from these and their neighboring images. For each of the two resulting images, a new center for the LV activity structure is defined by the center of gravity of the activity distribution within the contour detected by the fixed-ROI method. The ED and ES contours are then established for these images with the described minimum-cost approach. Figure 7 shows the detected contours in the original ED and ES images.

Using the average background count/pixel already computed, the EF by dual ROI for the study of Fig. 5 was found to be 46%, thus 10 units higher than the fixed-ROI EF in this case.

Ejection fraction by the variable-ROI method. With the dual-ROI method the ED and ES contours are detected in the corresponding frames without making any use of the temporal information available in the frames of the study. This information can be used to advantage through detecting the contours in the separate frames. An additional advantage from this approach accrues from the fact that instantaneous regional wall position may be assessed. This use of the separate frames is denoted the variable-ROI method. For the computation of the EF, the ED and ES count data can then be selected from the resulting time-activity curve. The S:N ratio in the separate frames is improved by 1-2-1-weighted temporal filtering of the consecutive frames. For the detection of the LV contour in frame m, the detected contour in frame (m-1) is used as a model to guide the search, i.e., a narrow expectation window can be defined. The contour detected in a new sum image constructed from the first six frames (representing 30% of the entire representative cycle) is used as a guide for the first frame of the study. For each subsequent frame to be analyzed, the centroid of the activity distribution within the region defined by the contour in the previous frame is defined as the new center position. Thus an adaptive process for the definition of the center positions is applied for each of the 20 frames. Minimal-cost contour detection is then applied to each of the separate frames.

From the time-activity curve, corrected for average background by the previously determined count/pixel, the EF following this variable-ROI method was found to be 50% for the foregoing example.

REFERENCES

1. PARKER JA, SECKER-WALKER R, HILL R, et al: A new technique for the calculation of left ventricular ejection fraction. *J Nucl Med* 13:649-651, 1972
2. GREEN MV, BRODY WR, DOUGLAS MA, et al: Ejection fraction by count rate from gated images. *J Nucl Med* 19: 880-883, 1978
3. DOUGLAS MA, GREEN MV, OSTROW HG: Evaluation of automatically generated left ventricular regions of interest in computerized ECG-gated radionuclide angiocardiography. Proc Comp in Card, IEEE Cat. No. 78CH1391-2C, pp 201-204, 1978
4. KAN MK, HOPKINS GB: Edge enhancement of ECG-gated cardiac images using directional masks. *Radiology* 127: 525-528, 1978
5. ALMASI JJ, BORNSTEIN I, EISNER RL, et al: Enhanced clinical utility of nuclear cardiology through advanced computer processing methods. Proc Comp in Card, IEEE Cat. No. 79CH1462-1C, pp 397-400, 1979
6. CHANG W, HENKIN RE, HALE DJ, et al: Methods for detection of left ventricular edges. *Semin Nucl Med* 10:39-53, 1980
7. HAWMAN EG: Digital boundary detection techniques for the analysis of gated cardiac scintigrams. *Optical Engineering* 20(5):719-725, 1981
8. BOURGUIGNON MH, DOUGLAS KH, LINKS JM, et al: Fully automated data acquisition, processing and display in equilibrium radioventriculography. *Eur J Nucl Med* 6: 343-347, 1981
9. LINKS J, BROWN G, HALL D, et al: A new method of fully-automated processing of gated blood pool studies. *J Nucl Med* 23:P85, 1982 (abst)
10. FESER JA: Automatische bestimmung der auswurffraktion des linken herzventrikels. *Röntgenstrahlen* 47:4-7, 1982
11. BUROW RD, STRAUSS HW, SINGLETON R, et al: Analysis of left ventricular function from multiple gated acquisition cardiac blood pool imaging. Comparison to contrast angiography. *Circulation* 56:1024-1028, 1977
12. OKADA RD, KIRSHENBAUM HD, KUSHNER FG, et al: Observer variance in the qualitative evaluation of left ventricular wall motion and the quantitation of left ventricular ejection fraction using rest and exercise multigated blood pool imaging. *Circulation* 61:128-136, 1980
13. LIE SP, REIBER JHC, HOEK C, et al: Automated boundary extraction from cardiac scintigrams. Proceedings VII International Conference on Image Processing in Medical Imaging, Stanford, June 22-26, 1981:310-328
14. GERBRANDS JJ, HOEK C, REIBER JHC, et al: Automated left ventricular boundary extraction from technetium-99m

gated blood pool scintigrams with fixed or moving regions of interest. Proc 2nd Int. Conf. on Visual Psychophysics and Medical Imaging, IEEE Cat. No. 81CH1676-6, pp 155-159, 1981.

15. GERBRANDS JJ, HOEK C, REIBER JHC, et al: Minimum cost contour detection in technetium-99m gated cardiac blood pool scintigrams. Proc Comp in Card, IEEE Cat. No. 81CH1750-9, pp 281-284, 1981
16. ASHBURN WL, SCHELBERT HR, VERBA JW: Left ventricular ejection fraction—A review of several radionuclide angiographic approaches using the scintillation camera. *Prog Cardiovasc Dis* XX:267-284, 1978
17. SILBER S, SCHWAIGER M, KLEIN U, et al: Quantitative Beurteilung der linksventrikularen Funktion mit der Radionuklid-Ventrikulographie. Bestimmung der globalen Auswurffraktion nach verschiedenen Auswerteverfahren, Erfassung der regionalen Auswurffraktion nach der radiärsegmentalen Methode. *Herz* 5:146-158, 1980
18. TAYLOR DN, GARVIE NW, CHIR B, et al: The effect of various background protocols on the measurement of left ventricular ejection fraction in equilibrium radionuclide angiography. *Br J Radiol* 53:205-209, 1980
19. SORENSEN SG, HAMILTON GW, WILLIAMS DL, et al: R-wave synchronized blood-pool imaging. A comparison of the accuracy and reproducibility of fixed and computer-automated varying regions-of-interest for determining the left ventricular ejection fraction. *Radiology* 131:473-478, 1979
20. KNAPP WH: The present state of isotope methods for evaluation of cardiac dynamics. Report Working Group of Nuclear Cardiology, European Society of Cardiology. Abstract book Workshop: Use of Isotopes. Tours: 40-48, 1979
21. CHAITMAN BR, DEMOTS H, BRISTOW JD, et al: Objective and subjective analysis of left ventricular angiograms. *Circulation* 52:420-425, 1975
22. ROGERS WJ, SMITH LR, HOOD WP, et al: Effect of filming projection and interobserver variability on angiographic biplane left ventricular volume determination. *Circulation* 59:96-104, 1979
23. BACHARACH SL, GREEN MV, SCHIEPERS CW, et al: Theoretical behavior of fixed and varying ROI methods for calculating EF. *J Nucl Med* 22:P60, 1981 (abst)
24. BUROW RD, STRAUSS HW, SINGLETON R, et al: Analysis of left ventricular function from multiple gated acquisition cardiac blood pool imaging. Comparison to contrast angiography. *Circulation* 56:1024-1028, 1977
25. KARSCH KR, SCHICHA H, RENTROP P, et al: Validity of different gated equilibrium blood pool methods for determination of left ventricular ejection fraction. *Eur J Nucl Med:* 439-445, 1980
26. PFISTERER ME, BATTLER A, SWANSON SM, et al: Reproducibility of ejection-fraction determinations by equilibrium radionuclide angiography in response to supine bicycle exercise: Concise communication. *J Nucl Med* 20:491-495, 1979
27. SLUTSKY R, KARLINER J, BATTLER A, et al: Reproducibility of ejection fraction and ventricular volume by gated radionuclide angiography after myocardial infarction. *Radiology* 132:155-159, 1979
28. WACKERS FJTh, BERGER HJ, JOHNSTONE DE, et al: Multiple gated cardiac blood pool imaging for left ventricular ejection fraction: validation of the technique and assessment of variability. *Am J Cardiol* 43:1159-1166, 1979
29. ASHKAR GP, MODESTINO JW: The contour extraction problem with biomedical applications. *Comp Graphics Image Proc* 7:331-355, 1978